Nanoscale

Accepted Manuscript

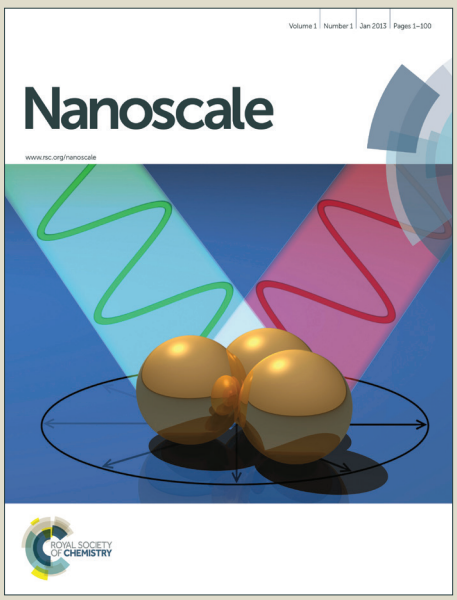

ROYAL SOCIETY OF CHEMISTRY

www.rsc.org/nanoscale

Cite this: DOI: 10.1039/c0xx00000x

www.rsc.org/xxxxxx

Paper

Broadband laser polarization control with aligned carbon nanotubes

He Yang[a†], Bo Fu[a,b†], Diao Li[a,c†], Ying Tian[d], Ya Chen[a], Marco Mattila[a], Zhenzhong Yong[e], Ru Li[e], Abdou Hassanien[f], Changxi Yang[b], Ilkka Tittonen[a], Zhaoyu Ren[c], Jingtao Bai[c], Qingwen Li[e], Esko I. Kauppinen[d], Harri Lipsanen[a], and Zhipei Sun[a]*

Received (in XXX, XXX) Xth XXXXXXXXX 20XX, Accepted Xth XXXXXXXXX 20XX
DOI: 10.1039/b000000x

We introduce a simple approach to fabricate aligned carbon nanotube (ACNT) device for broadband polarization control in fiber laser systems. The ACNT device was fabricated by pulling from as-fabricated vertically-aligned carbon nanotube arrays. Their anisotropic property is confirmed with various microscopies. The device was then integrated into fiber laser systems (at two technologically important wavelengths of 1 and 1.5 μm) for polarization control. We obtained a linearly-polarized light output with the maximum extinction ratio of ~12 dB. The output polarization direction could be fully controlled by the ACNT alignment direction in both lasers. To the best of our knowledge, this is the first time that ACNT device is applied to polarization control in laser systems. Our results exhibit that the ACNT device is a simple, low-cost, and broadband polarizer to control laser polarization dynamics, for various photonic applications (such as material processing, polarization diversity detection in communications), where the linear polarization control is necessary.

1. Introduction

Carbon nanotubes (CNTs)[1] have been extensively investigated due to their inherent physical properties (e.g., electrical,[2] optical,[3] and thermal[4,5] properties), enabling various applications, such as electron field emitters,[6] quantum resistors,[7] transistors,[8] atomic force microscopes,[9] mechanical memory elements,[10] etc.[11-15] Worth noting that, CNTs have recently attracted huge attention for various photonic and optoelectronic applications[2] because of their unique optical properties, such as broadband optical absorption,[16-18] large optical nonlinearity,[19] ultrafast carrier relaxation time,[20] and high damage threshold.[21] One of the most successful examples is CNT-based saturable absorber,[22,23] which has been employed for ultrafast pulse generation in solid-state,[24] semiconductor,[25] waveguide,[26] and fiber lasers.[27]

Due to the unique structure confinement in one-dimension, aligned CNTs (ACNT) have been demonstrated to facilitate a large range of applications (such as touch screen,[28] solar cells,[29] sensors,[30] supercapacitors,[31] thermal interface materials,[32] batteries,[33] infrared and THz sources/detection,[34-36] and anisotropic saturable absorbers[37,38]), underscoring superior performance compared to their randomly oriented counterpart. In particular, ACNTs have strong optical anisotropic characteristic,[39,40] enabling polarizer applications with superior performance when compared to the conventional bulk polarizers (e.g., prisms and fiber Bragg grating (FBG) [41,42]), such as easy fabrication, broad operation bandwidth (from ultraviolet,[18] visible,[43] infrared,[44] to THz range[45,46]), and high extinction ratio (up to 30 dB[44]).

Laser polarization control is very crucial for a large range of photonic applications, ranging from fluorescence imaging, liquid crystal device characterization and manufacturing, to laser material processing and polarization diversity detection in communications and range finding. In this paper, we introduce a simple technique to fabricate ACNT device, by which broadband (at 1 and 1.5 μm) laser polarization dynamics is fully controlled after integration into fiber laser systems. The maximum extinction ratio of ~12 dB is achieved. To the best of our knowledge, it is the first time that such ACNT device is applied to the fiber laser systems for polarization control. Our study demonstrates the unique broadband performance of ACNTs for various photonics and optoelectronics applications.

2. Fabrication and characterization of the ACNT device

The ACNT device was made by pulling out from a vertically-aligned CNT array,[30] which was fabricated with chemical vapour deposition method.[47] Then the ACNT film was directly transferred onto the surface of a quartz substrate (as shown in Fig. 1 (a) after inserting into a mirror mount). Note that our direct-dry

[a] *Department of Micro- and Nanosciences, Aalto University, PO Box 13500, FI-00076 Aalto, Finland. E-mail: zhipei.sun@aalto.fi; Tel: +358-50-4322979*
[b] *The State Key Laboratory of Precision Measurement Technology and Instruments, Department of Precision Instruments, Tsinghua University, Beijing 100084, China*
[c] *Institute of Photonics and Photo-Technology, School of Physics, Northwest University, Xi'an, Shaanxi 710069, China*
[d] *Department of Applied Physics, Aalto University School of Science, PO Box 15100, FI-00076 Aalto, Finland*
[e] *Institute of Nano-tech and Nano-bionics, Chinese Academy of Sciences, Suzhou, Jiangsu 215125, China*
[f] *National Institute of Chemistry, 19 Hajdrihova, Ljubljana 1000, Slovenia*
† He Yang, Bo Fu and Diao Li contributed equally to this work.

transfer fabrication method is also compatible to other photonic devices (e.g., fibers and silicon devices).

In order to characterize the alignment performance, various microscopies were utilized, such as optical microscopy (Fig. 1(b)), and scanning electron microscopy (SEM, Fig. 1(c)). As shown in the figure, CNT arrays were highly-aligned along the pulling direction. The diameter of the CNTs was measured to be ~ 5 nm by transmission electron microscopy (TEM, Fig. 1 (d)). It denotes that our sample consists typically of few-wall CNTs.

In order to achieve the best polarization performance, we optimize the output performance with different film thicknesses (from ~100 nm to ~300 nm), shown in Fig. S1 of Supporting Information. We find that thicker samples give better performance, and the output performance (e.g., extinction ratio (ER)) saturates when the thickness is ~ 300 nm. Therefore, ~300 nm ACNT film is selected in our experiment.

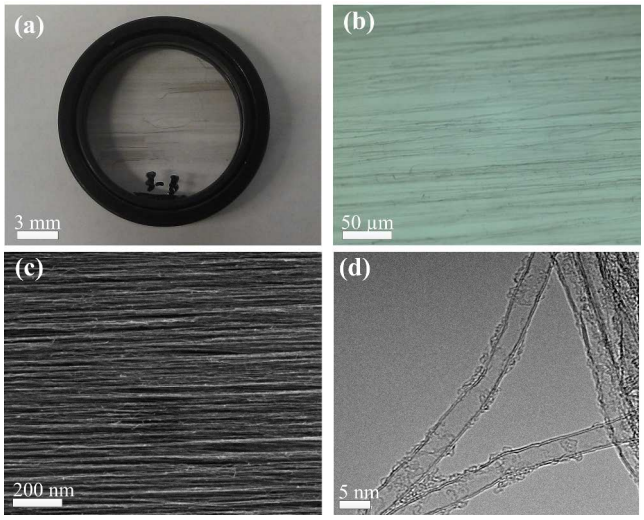

Fig. 1 (a) ACNT on 1-inch quartz substrate, (b) its optical microscope image, (c) SEM image and (d) TEM image.

For ACNTs, their Raman scattering intensity varies with different excitation polarization direction. In our experiment, a polarized Raman spectroscopy (WITec Alpha 300 RA) was utilized to characterize the anisotropic properties of the ACNT samples. Polarized Raman spectra were conducted by changing the input polarization direction (ϕ) of the excitation laser from 0° to 360° with respect to the CNT alignment direction. When ϕ=0° and ϕ=90°, the incident excitation polarization direction is parallel and perpendicular to the ACNT alignment direction, respectively. Typical Raman spectra (Fig. 2 (a)) showed three dominating features, namely D, G, and G' modes, as typically observed for few-wall carbon nanotubes.[48,49] It has been reported that the G-band of Raman modes at around 1580 cm^{-1} is highly sensitive to CNTs alignment.[48] When we change the angle ϕ, the intensity of G-peak and D-peak changes from the maximum (at ϕ=0°) to the minimum (at ϕ=90°), which was in accordance with the polarized absorbance of the aligned carbon nanotube.[50,51] The ratio between the maximum and the minimum intensity is ~22. In our study, the G-peak intensity at different angle ϕ is presented in Fig. 2 (b). It indicates that the Raman scattering intensity of ACNTs is sensitive to the polarization direction of the pump light, well agreeing with the equation of $I(\phi) \propto \cos^2(\phi)$[48] for ACNTs. Such anisotropic Raman property clearly shows that CNTs are well aligned.

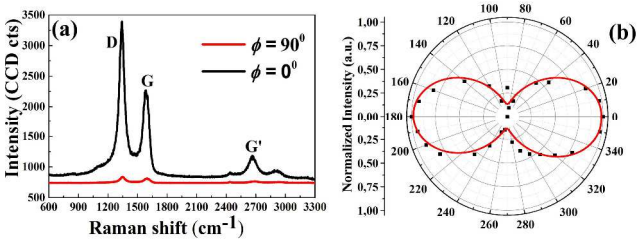

Fig. 2 (a) Polarized Raman spectra of the ACNT device, (b) G-peak Raman intensity as a function of the angle, and the red line depicts the fitting result with the equation. The excitation laser wavelength is 532 nm.

Fig. 3 (a) shows the polarized transmittance of our ACNT device in the two orthogonal directions (i.e., when the polarization direction of the input light is parallel or perpendicular to the CNT alignment direction), which is measured by a polarized absorption spectroscopy. When the incident light polarization is perpendicular to the ACNT alignment direction, the transmittance is ~94% at 1.8 μm, which is mainly contributed by Fresnel loss (~6%) of the quartz substrate. While for the parallel polarization light input, the transmittance is ~82% at 1.8 μm. The result identifies the optical anisotropic absorption of our CNT device. The difference between two orthogonal directions is ~12% at 1.8 μm (~16% at 300 nm, as shown in Fig. 3 (b)), which is comparable to the typical performance reported for aligned carbon nanotubes (from 15% to 20% at different wavelengths[43,44]). Note that the transmittance difference remains almost constantly from 1 to 2 μm, which shows the unique broad operation bandwidth of our device. For comparison, the transmittance difference at parallel and perpendicular directions of a pure quartz reference sample (3 mm thick) was also tested. The result shows that the anisotropic absorption of our ACNT device is merely contributed by the ACNTs.

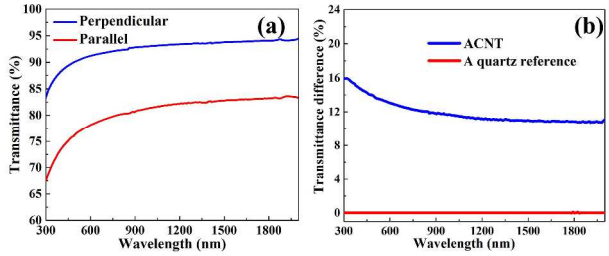

Fig. 3 (a) Polarized transmittance of the ACNT device with the aligned direction parallel and perpendicular to the polarization direction of the incident light source, respectively. (b) The transmittance difference in the two orthogonal directions for ACNT device and pure quartz.

3. Laser setup

To utilize the broadband anisotropic characteristics of the ACNT device, fiber lasers operating at 1 and 1.5 μm were designed with identical layout (Fig. 4 (a)). In the fiber laser at 1.5 μm: a 1 m erbium doped (Er-doped) fiber worked as the gain fiber, a wavelength division multiplexer (WDM) was used to couple the pump laser (980 nm laser diode (LD)) into the gain fiber, the ACNT device was inserted inside a fiber-collimator based U-bench to modulate the intra-cavity polarization state, a high-reflectivity fiber based mirror (made by a 3-dB coupler as a nonlinear optical loop mirror) was provided for laser feedback,

while a fiber coupler with 20% coupling ratio outputs the laser from the cavity for measurement. In the 1-μm fiber laser: the gain fiber was replaced by 0.5 m ytterbium doped (Yb-doped) fiber, and other components (e.g., WDM, LD, and coupler) with same function were selected at 1 μm. In both laser systems, all fiber components were polarization independent, indicating no intra-cavity polarization preference without ACNTs.

An optical spectrum analyser (Hewlett Packard, 86140A) was utilized to measure the laser output spectrum. A polarization analyser (i.e., a linear polarizer) mounted in a high-precision rotator was fixed after the output coupler, illustrated in Fig. 4 (b), to characterize the laser polarization output performance. By rotating the angle (marked as φ in Fig. 4 (b)) between the axis (white line in Fig. 4 (b)) of the polarization analyzer and the vertical direction (dotted line) from 0˚ to 360˚, the output laser power after the analyzer was monitored by a power meter (OPHIR Nova II) to characterize the output polarization state.

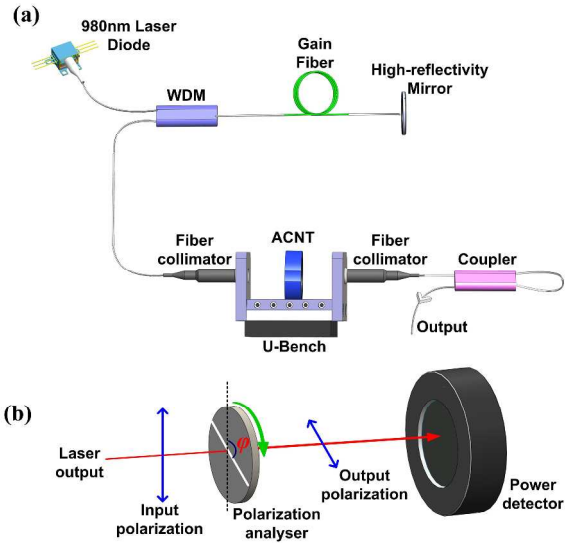

Fig. 4 (a) Fiber laser setup for both 1 and 1.5 μm laser systems, (b) laser polarization performance characterization system.

4. Polarization control results and discussions

4.1 1.5 μm Er-doped fiber laser (EDFL)

In EDFL, continuous wave output performance was studied with a pure quartz as a reference or our ACNT device in the U-bench (Fig. 4 (a)). Fig. 5 (a) shows the typical output optical spectrum, identical for both cases (with the quartz reference and the ACNT device). The peak wavelength is ~1561 nm with the full width at half maximum (FWHM) of 0.1 nm, a typical value for such erbium-doped fiber laser without mode-selection. The output power as a function of the pump power is demonstrated in Fig. 5 (b). The output power presents linear characteristics for both situations, while the slope efficiency decreased when the ACNT device was inserted. It is because the ACNT device in the cavity also introduces additional small attenuation to the laser cavity. The laser threshold of pump power was ~34 mW. The maximum output power decreased from ~2.0 to ~1.6 mW under the highest pump power of ~180 mW (the maximum output power from the laser diode), after replacing the quartz reference with the ACNT device in the cavity. Further increase of the laser output power is possible, as the output power linearly increases with the pump power with no sign of saturation.

To investigate the polarization dynamics of our ACNT device in the laser resonator, we experimentally measured the laser output power after the polarization analyzer, as shown in Fig. 4- (b). At first, we inserted the ACNT device into the laser resonator and fixed the alignment direction of ACNT vertical to the horizontal plane in the free space, without changing any experimental conditions. After that, the output laser power after the polarization analyzer angle was recorded by changing the angle φ *(shown in Fig. 4 (b))* from 0˚ to 360˚. The experimental results are illustrated in Fig. 5(c), fitted well with the cosine function, i.e., the minimum output power was close to zero at the angle of 0˚, while the maximum power located at the angle of 90˚. It shows that the output polarization of the laser was changed from the random-polarization state to the linear-polarization state, after insertion of our ACNT device in the laser cavity. In order to fully study the performance of intra-cavity polarization control of ACNT device, the CNT alignment direction was rotated from vertical to horizontal orientation for comparison. The corresponding results are also shown in Fig. 5 (c). It is observed that the whole curve shifts 90˚ when comparing to the one with vertical orientation of the ACNT device. The result suggests that the laser output with ACNT device was linearly-polarized, and the polarization direction rotates with the rotation of the ACNT device. This shows that the polarization state of our laser output can be simply controlled by rotating the intra-cavity ACNT device. Fig. 5(d) summarizes the degree of polarization (DOP) and ER of our ACNT laser versus pump power. The DOP and ER are defined as $DOP=(P_{max}-P_{min})/(P_{max}+P_{min})$, $ER=P_{max}/P_{min}$, where P_{max} and P_{min} are the maximum and minimum output power given by the measured results shown in Fig. 5 (c). The maximum DOP of our ACNT laser is 87.5% at the pump power of ~75 mW, 10-time higher than the DOP of the laser with the quartz reference (~8%, as shown in the inset of Fig. 5(d)). The corresponding ER of our ACNT laser is ~12 dB, around 8-time higher than the value of the laser with the quartz reference (~1.5 dB). The ER is ~9.8 dB (with 81% of DOP) at the maximum output power of 1.6 mW. The DOP and ER performance is pretty unchanging when the pump power is high (>100 mW). This is because the anisotropic absorption of ACNT dominates the laser output polarization performance at the high pump power. No performance degradation is observed during 1.5 hours experiment. We also carry out the same polarization control experiment with a traditional prism based polarizer (Thorlabs, GL10) for comparison. The comparison results are given in Fig. S2 of Supporting Information, which shows that the polarization performance of our ACNT laser is comparable (~ 8% difference) to the laser using the traditional prism based polarizer. Worth noting that our ACNT fabrication method is compatible to other photonic devices (e.g., fibers and silicon devices), which can offer huge flexibility to be integrated into various photonic platforms (e.g., waveguides) for a large range of photonics applications.

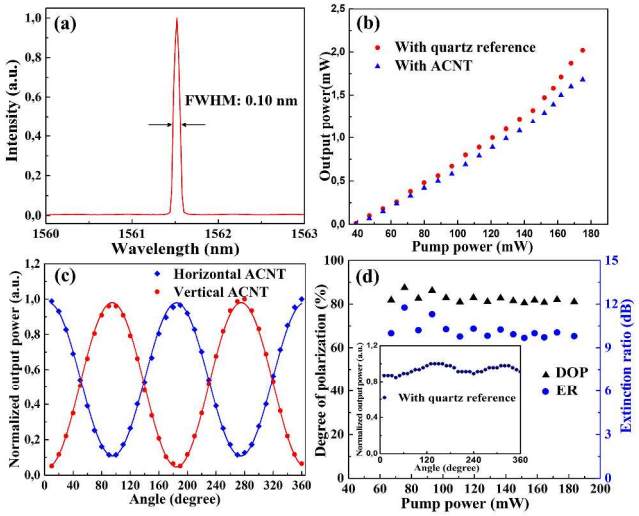

Fig. 5 Experimental results at 1.5 μm: (a) output spectrum (b) output power as a function of pump power (with the quartz reference and our ACNT device), (c) normalized output power as a function of polarization analyser angle of our ACNT laser output, and the cosine function fitting of the experimental data (d) DOP and ER versus pump power, and the inset figure is the normalized output power of the laser with a quartz reference as a function of polarization analyser angle.

4.2 1 μm Yb-doped fiber laser (YDFL)

In our ACNT based YDFL, the output spectrum is shown in Fig.-6 (a). The peak wavelength is ~1032 nm with FWHM of ~0.1 nm, typical for an YDFL without any wavelength selection component in the cavity. The spectrum is similar to the laser system with a quartz reference and our ACNT device. Fig. 6 (b) illustrates the results of laser output power under the conditions with the quartz reference and our ACNT device. The threshold for the laser system with ACNT (27 mW) was slightly higher than that (24 mW) with the quartz reference. With the increase of the pump power, the output power increased linearly. The highest output power for the laser with the quartz reference is ~3.2 mW, while for the laser with ACNT device, the output power is ~2.75 mW.

Fig. 6 (c) presents the polarization control results of our 1-μm YDFL with ACNT device. Similar to the EDFL experiment, we firstly inserted the ACNT device into the resonator, and used the experimental procedures (identical to what we employed in EDFL) to study the polarization state of the laser output. The result is given in Fig. 6 (c). As expected, the output of our laser with ACNT became linearly polarized, and the polarization state can be controlled by the rotation of the ACNT alignment direction. After, we also measured the laser output power change after the polarization analyzer with the quartz reference, as illustrated in the inset figure of Fig. 6 (d). The output power keeps almost unvarying with the fluctuation of ~ 5.8%, which indicates that the output of our laser with the quartz reference is randomly-polarized, similar to what we observed with the laser working at 1.5 μm. Fig. 6 (d) summarizes the DOP and ER versus pump power. The DOP reaches ~89% at the pump power of 59.4 mW (in contrast to the DOP of 2.9% with the quartz reference in the laser cavity). It decreased slightly as we increased the pump power, which also confirms good polarization dynamics control of our 1 μm fiber laser with the ACNT device. The maximum ER is ~ 12.4 dB, comparable to the result achieved with the EDFL.

Similarly, we conducted the polarization control experiment with the prism based polarizer (Thorlabs, GL10) for comparison, depicted in Supporting Information Fig. S2. The result illustrates that the polarization performance of our ACNT laser is comparable (~7% difference) to the one using the traditional prism based polarizer and also these typically published with FBGs (e.g., ER of 15 dB [42]). We also did not observe any device damage during our experiment.

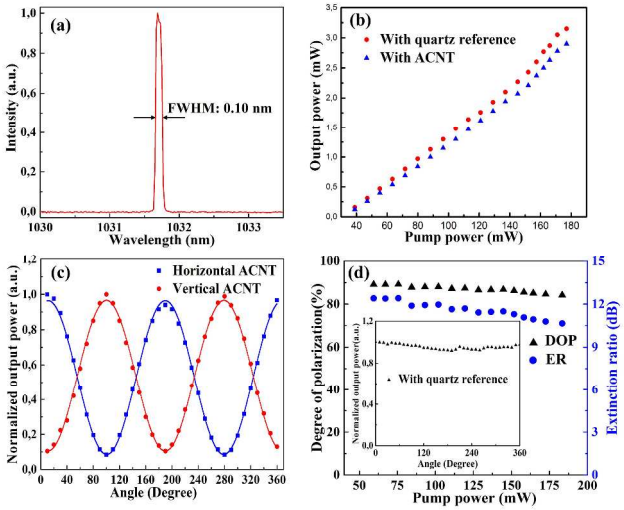

Fig. 6 Experimental results at 1 μm: (a) output spectrum, (b) output power as a function of pump power (with the quartz reference and our ACNT device), (c) normalized output power as a function of angle with the polarization analyser, and the cosine function fitting of the experimental data, (d) DOP and ER versus pump power, and the inset figure is the normalized output power of the laser with the quartz reference as a function of polarization analyser angle when the laser is with the quartz reference.

Conclusions

We introduce a simple method to fabricate ACNT device for broadband polarization control in laser systems (at 1 and 1.5 μm). The anisotropic property of ACNTs was confirmed with various characterization methods (e.g., optical microscopy, SEM, and Raman spectroscopy). By integrating the ACNT device into the filer laser system, we obtained a linearly-polarized light output with DOP up to 89.1% and 87.5% with corresponding ER of 12.4 and ~12 dB in 1 and 1.5 μm laser systems, respectively. Our experimental results exhibit that the ACNT device can be potentially employed as polarization controller for a broad range of photonic applications (nonlinear frequency conversion,[52,53] beam combination,[54] material processing and polarization diversity detection in communications etc.), where the linear polarization output is required.

Acknowledgements

The authors acknowledge funding from Teknologiateollisuus TT-100, Academy of Finland (grants: 276160, 276376, 284548,

285972), the European Union's Seventh Framework Programme (REA grant agreement No. 631610), National Natural Science Foundation of China (grant: 61377039, 61177059), China Scholarship Council, and Aalto University (Finland). The authors also thank the provision of facilities and technical support by Aalto University at Micronova Nanofabrication Centre.

Author contribution:

Z.S., H.Y., B.F. and D.L. conceived and designed the laser experiments. Z.S., Y.T., Y.C., and M.M. performed the characterization experiments. Z.Y. and Q.L. fabricated the ACNT device. R.L. performed the TEM measurement, A.H. performed the sample thickness measurement with AFM. I.T., Z.R., J.B., Q.L., E.K., H.L., and Z. S coordinated the experiments. All authors contributed to the writing of the manuscript and to the discussion.

Notes and references

1 S. Iijima, "Helical microtubules of graphitic carbon," *Nature,* 1991, **354,** 56–58.

2 P. Avouris, M. Freitag, and V. Perebeinos, "Carbon-nanotube photonics and optoelectronics," *Nat. Photon.,* 2008, **2,** 341–350.

3 M. S. Dresselhaus, A. Jorio, M. Hofmann, G. Dresselhaus, and R. Saito, "Perspectives on carbon nanotubes and graphene raman spectroscopy," *Nano Lett.,* 2010, **10,** 751–758.

4 V. N. Popov, "Carbon nanotubes: properties and application," *Mat. Sci. Eng. R Rep.,* 2004, **43,** 61–102.

5 C. N. R. Rao, B. C. Satishkumar, A. Govindaraj, and M. Nath, "Nanotubes," *Chem. Phys. Chem.,* 2001, **2,** 78–105.

6 A. G. Rinzler, J. H. Hafner, P. Nikolaev, P. Nordlander, D. T. Colbert, R. E. Smalley, L. Lou, S. G. Kim, D. Tománek, "Unraveling nanotubes: field emission from an atomic wire," *Science,* 1995, **269,** 1550–1553.

7 S. Frank, P. Poncharal, Z. L. Wang, and W. A. de Heer, "Carbon nanotube quantum resistors," *Science,* 1998, **280,** 1744–1746.

8 S. J. Tans, A. R. M. Verschueren, and C. Dekker, "Room-temperature transistor based on a single carbon nanotube," *Nature,* 1998, **393,** 49–52.

9 N. R. Wilson, and J. V. Macpherson, "Carbon nanotube tips for atomic force microscopy," *Nature Nanotech.,* 2009, **4,** 483–491.

10 H. Ko, Z. Zhang, J. C. Ho, K. Takei, R. Kapadia, Y. -L. Chueh, W. Cao, B. A. Cruden, and A. Javey, "Flexible carbon-nanofiber connectors with anisotropic adhesion properties," *Small,* 2010, **6,** 22–26.

11 P. L. McEuen, "Nanotechnology: carbon-based electronics," *Nature,* 1998, **393,** 15–17.

12 P. Avouris, "Molecular electronics with carbon nanotubes," *Acc. Chem. Res.,* 2002, **35,** 1026–1034.

13 H. Dai, J. H. Hafner, A. G. Rinzler, D. T. Colbert, and R. E. Smalley, "Nanotubes as nanoprobes in scanning probe microscopy," *Nature,* 1996, **384,** 147–150.

14 P. Kim, and C. M. Lieber, "Nanotube nanotweezers," *Science,* 1999, **286,** 2148–2150

15 B. Liu, C. Wang, J. Liu, Y. Che, and C. Zhou, "Aligned carbon nanotubes: from controlled synthesis to electronic applications," *Nanoscale*, 2013, **5,** 9483–9502.

16 F. Wang, A. G. Rozhin, V. Scardaci, Z. Sun, F. Hennrich, I. H. White, W. I. Milne, and A. C. Ferrari, "Wideband-tuneable, nanotube mode-locked, fibre laser," *Naure Nanotech*., 2008, **3,** 738–742.

17 Y. Murakami, E. Einarsson, T. Edamura, and S. Maruyamaet, "Polarization dependence of the optical absorption of single-walled carbon nanotubes," *Phys. Rev. Lett.,* 2005, **94,** 087402.

18 S. Kivistö, T .Hakulinen, A. Kaskela, B. Aitchison, D. P. Brown, A. G. Nasibulin, E. I. Kauppinen, A. Härkönen, and O. G. Okhotnikov, "Carbon nanotube films for ultrafast broadband technology," *Opt. Express,* 2009, **17,** 2358–2363.

19 W. B. Cho, J. H. Yim, S. Y. Choi, S. Lee, A. Schmidt, G. Steinmeyer, U. Griebner, V. Petrov, D.-I. Yeom, K. Kim, and F. Rotermund, "Boosting the nonlinear optical response of carbon nanotube saturable absorbers for broadband mode-locking of bulk lasers," *Adv. Funct. Mater.,* 2010, **20,** 1937–1943.

20 Martinez, and Z. Sun, "Nanotube and graphene saturable absorbers for fibre lasers," *Nature Photon.,* 2013, **7,** 842–845.

21 Z. Sun, A.G. Rozhin, F. Wang, T. Hasan, D. Popa, W. O'Neill, A. C. Ferrari, "A compact, high power, ultrafast laser mode-locked by carbon nanotubes," *Appl. Phys. Lett.,* 2009, **95,** 253102.

22 Z. Sun, T. Hasan, and A. C. Ferrari, "Ultrafast lasers mode-locked by nanotubes and graphene," *Physica E.* 2012, **44,** 1082–1091.

23 T. Hasan, Z. Sun, F. Wang, F. Bonaccorso, P. H. Tan, A. G. Rozhin, and A. C. Ferrari, "Nanotube-Polymer Composites for Ultrafast Photonics," *Adv. Mater*., 2009, **21,** 3874–3899.

24 W. B. Cho, J.H. Yim, S.Y. Choi, S. Lee, U. Griebner, V. Petrov, F. Rotermund, "Mode-locked self-starting Cr:forsterite laser using a single-walled carbon nanotube saturable absorber," *Opt. Lett.,* 2008, **33,** 2449–2451.

25 Y. W. Song, S. Yamashita, C. S. Goh, S. Y. Set, "Passively mode-locked lasers with 17.2-GHz fundamental-mode repetition rate pulsed by carbon nanotubes," *Opt. Lett.,* 2007, **32,** 430–432.

26 G. Della Valle, R. Osellame, G. Galzerano, N. Chiodo, G. Cerullo, P. Laporta, O. Svelto, U. Morgner, A.G. Rozhin, V. Scardaci, A.C. Ferrari, "Passive mode locking by carbon nanotubes in a femtosecond laser written waveguide laser," *Appl. Phys. Lett.,* 2006, **89,** 231115.

27 S. Y. Set, H. Yamaguchi, Y. Tanaka, M. Jablonski, Y. Sakakibara, A. Rozhin, M. Tokumoto, H. Kataura, Y. Achiba, and K. Kikuchi, "Mode-locked fiber lasers based on a saturable absorber incorporating carbon nanotubes," *Optical Fiber Communication Conference,* 2003, PD44.

28 K. L. Jiang, J. P. Wang, Q. Q. Li, L. Liu, C. H. Liu, and S. S. Fan, "Superaligned carbon nanotube arrays, films, and yarns: a road to applications," *Adv. Mater.,* 2011, **23,** 1154-1161.

29 T. Hasobe, S. Fukuzumi, and P. V. Kamat, Stacked-cup carbon nanotubes for photoelectrochemical solar cells," *Angew. Chem. Int. Edit.,* 2006, **45,** 755–759.

30 R. H. Baughman, A. A. Zakhidov, and W. A. de Heer, "Carbon nanotubes-the route toward applica-tions," *Science,* 2002, **297,** 787–792.

31 T. Chen, H. Peng, M.l Durstock, and L. Dai, "High-performance transparent and stretchable all-solid supercapacitors based on highly aligned carbon nanotube sheets," *Sci. Rep.,* 2014, **4,** 3612.

32 X. J. Hu, A. A. Padilla, J. Xu, T. S. Fisher, and K. E. Goodson, "3-omega measurements of vertically oriented carbon nanotubes on silicon," *J. Heat Transf.,* 2006, **128,** 1109–1113.

33 X. Cheng, J. Huang, Q. Zhang, H. Peng, M. Zhao, and F. Wei, "Aligned carbon nanotube/sulfur composite cathodes with high sulfur content for lithium-sulfur batteries," *Nano Energy,* 2014, **4,** 65–72.

34 L. Ren, Q. Zhang, C. L. Pint, A. K. W´ojcik, M. Bunney, Jr., T. Arikawa, I. Kawayama, M. Tonouchi, R. H. Hauge, A. A. Belyanin, and J. Kono, "Collective antenna effects in the terahertz and infrared response of highly aligned carbon nanotube arrays," *Phys. Rev. B,* 2013, **87,** 161401(R).

35 X. W. He, X. Wang, S. Nanot, K. Cong, Q. J. Jiang, A. A. Kane, J. E. M. Goldsmith, R. H. Hauge, R. Leonard, and J. Kono, "Photothermoeletric p-n junction photodetector with intrinsic broadband polarimetry based on macroscopic carbon nanotube films," *ACS Nano,* 2013, **7**, 7271–7277.

36 X. W. He, N. Fujimura, J. M. Lloyd, K. J. Erickson, A. A. Talin, Q. Zhang, W. L. Gao, Q. J. Jiang, Y. Kawano, R. H. Hauge, R. Leonard, and J. Kono, "Carbon Nanotube Terahertz Detector," *Nano Lett*., 2014, **14**, 3953–3958.

37 A. G. Rozhin, Y. Sakakibara, H. Kataura, S. Matsuzaaki, K. Ishida, Y. Achiba, M. Tokumoto, ''Anisotropic saturable absorption of single wall carbon nanotubes aligned in polyvinyl alcohol,'' *Chem. Phys. Lett.*, 2005, **405**, 288–293.

38 A.G. Rozhin, Y. Sakakibara, M. Tokumoto, H. Kataura, Y. Achiba, ''Near-infrared nonlinear optical properties of single-wall carbon nantotubes embedded in polymer film,'' *Thin solid films*, 2004, **464–465**, 368–372.

39 Z. Ren, Y. Lan, and Y. Wang, "Aligned Carbon Nanotubes," *NanoScience and Technology, Springer,* 2013.

40 W. A. deHeer, W. S. Bacsa, A. Châtelain, T. Gerfin, R. Humphrey-Baker, L. Forro, and D. Ugarte, "Aligned Carbon Nanotube Films: Production and Optical and Electronic Properties," *Science*, 1995, **268,** 845–847.

41 N. Jovanovic, J. Thomas, R. J. Williams, M. J. Steel, G. D. Marshall, A. Fuerbach, S. Nolte, A. Tunnermann, and M. J. Withford, ''Polarizaation-dependent effects in point-by-point fiber Bragg gratings enalbe simple, linearly polarized fiber lasers,'' *Opt. Express*, 2009, **17**, 6082–6095.

42 J. H. Wang, J. M. Hu, L. Zhang, X. J. Gu, J. B. Chen, and Y. Feng, ''A 100W all-fiber linearly-polarized Yb-doped single-mode fiber laser at 1120 nm,'' *Opt. Express*, 2012, **20**, 28373–28378.

43 S. Shoji, H. Suzuki, R. P. Zaccaria, Z. Sekkat, and S. Kawata, "Optical polarizer made of uniaxially aligned short single-wall carbon nanotubes embedded in a polymer film," *Phys. Rev. B,* 2008, **77,** 153407.

44 L. Ren, Q. Zhang, C. L. Pint, A. K. W´ojcik, M. Bunney, Jr., T. Arikawa, I. Kawayama, M. Tonouchi, R. H. Hauge, A. A. Belyanin, and J. Kono, "Collective antenna effects in the terahertz and infrared response of highly aligned carbon nanotube arrays," *Phys. Rev. B,* 2013, **87,** 161401(R).

45 L. Ren, C. L. Pint, T. Arikawa, K. Takeya, I. Kawayama, M. Tonouchi, R. H. Hauge, and J. Kono, "Broadband terahertz polarizers with ideal performance based on aligned carbon nanotube stacks," *Nano Lett.,* 2012, **12,** 787–790.

46 L. Ren, C. L. Pint, L. G. Booshehri, W. D. Rice, X. Wang, D. J. Hilton, K. Takeya, I. Kawayama, M. Tonouchi, R. H. Hauge, and J. Kono, "Carbon nanotube terahertz polarizer," *Nano Lett.,* 2009, **9,** 2610–2613.

47 J. Di, Z. Yong, X. Zheng, B. Sun, and Q. Li, "Aligned carbon nanotubes for high-efficiency schottky solar cells," *Small,* 2013, **9,** 1367–1372.

48 G. S. Duesberg, I. Loa, M. Burghard, K. Syassen, and S. Roth, "Polarized Raman spectroscopy on isolated single-wall carbon nanotubes," *Phys. Rev. Lett.,* 2000, **85,** 5436.

49 A. M. Rao, A. Jorio, M. A. Pimenta, M. S. S. Dantas, R. Saito, G. Dresselhaus, and M. S. Dresselhaus, "Polarized Raman study of aligned mutiwalled carbon nanotubes," *Phys. Rev. Lett.,* 2000, **84,** 1820–1823.

50 M. S. Dresselhaus, G. Dresselhaus, A. Jorio, A. G. SouzaFilho, and R. Saito, "Raman spectroscopy on isolated single wall carbon nanotubes," *Carbon,* 2002, **40,** 2043–2061.

51 H. H.Gommand, J. W. Alldredge, H. Tashiro, J. Park, J. Magnuson, and A. G. Rinzler, "Fibers of aligned single-walled carbon nanotubes: Polarized Raman spectroscopy," *J. Appl. Phys.,* 2000, **88,** 2509–2514.

52 Z. Sun, R. Li, Y. Bi, X. Yang, G. Wang, W. Zhao, H. Zhang, W. Hou, D. Cui, and Z. Xu, "Generation of 11.5 W coherent red-light by intra-cavity frequency-doubling of a side-pumped Nd:YAG laser in a 4-cm LBO," *Opt. Commun.,* 2004, **241,** 167–172.

53 Z. Sun, and A. C. Ferrari, "Fibre sources in the deep ultraviolet," *Nature Photon.,* 2011, **5,** 446–447.

54 Q. Peng, Z. Sun, Y. Chen, L. Guo, Y. Bo, X. Yang, and Z. Xu, "Efficient improvement of laser beam quality by coherent combining in an improved Michelson cavity," *Opt. Lett.,* 2005, **30,** 1485–1487.